

Stokes theory of thin-film rupture

D. Moreno-Boza, A. Martínez-Calvo, and A. Sevilla*

Grupo de Mecánica de Fluidos, Departamento de Ingeniería Térmica y de Fluidos,
Universidad Carlos III de Madrid. Avda. de la Universidad 30, 28911, Leganés, Madrid, Spain.

(Dated: June 12, 2019)

The structure of the flow induced by the van der Waals destabilization of a non-wetting liquid film placed on a solid substrate is unraveled by means of theory and numerical simulations of the Stokes equations. Our analysis reveals that lubrication theory, which yields $h_{\min} \propto \tau^{1/5}$ where h_{\min} is the minimum film thickness and τ is the time until breakup, cannot be used to describe the local flow close to rupture. Instead, the slender lubrication solution is shown to experience a crossover to a universal self-similar solution of the Stokes equations that yields $h_{\min} \propto \tau^{1/3}$, with an opening angle of 37° off the solid.

A non-wetting liquid film placed on a solid substrate becomes unstable to infinitesimal surface waves when its thickness becomes smaller than about 100 nm, leading to a spinodal dewetting pathway coexistent with hole nucleation [1–9]. Spontaneous growth of perturbations takes place when the destabilizing van der Waals (vdW) forces exceed the stabilizing surface tension force, provided that the disturbance wavenumber is below a certain cut-off [10–12]. Previous theoretical efforts to describe the nonlinear dynamics leading to film rupture were based on lubrication theory [9, 13, 14], which assumes that the longitudinal length scale is much larger than the film thickness, and provides models with simpler mathematical structure than the Navier-Stokes equations. Indeed, while the latter must be solved as a free boundary problem where the film thickness h is part of the solution, the former leads to a partial differential equation (PDE) for h as a function of the relevant spatial coordinates and time, that is physically transparent and more amenable to analysis.

In this Letter, through dimensional arguments, numerical computations and similarity theory, we reveal that the Stokes flow close to the rupture singularity provides results markedly different from previous ones based on lubrication theory [14]. Our local theory, motivated by dimensional analysis, is inspired by pioneering studies of singularities in free-surface flows without resorting to one-dimensional approximations of the equations of motion, in contexts like the breakup of liquid jets [15, 16], or the ejection of jets from Faraday waves [17].

Flow configuration.— Consider a planar film of Newtonian liquid of viscosity μ coating a solid surface that spans the (x, z) plane. As sketched in Fig. 1 the film, of initial height h_o , is surrounded by a passive gaseous atmosphere at constant pressure, such that the gas-liquid interface has a surface tension σ , and is described by the function $y = h(x, t)$. The liquid film, initially at rest, becomes unstable due to the long-range vdW forces, whose collective effects are modeled through a disjoining pressure, $A/(6\pi h^3)$, with associated Hamaker constant A [18], being $A > 0$ in the non-wetting case considered herein. The latter intermolecular force model, which considers only non-retarded vdW interactions, is the simplest one among a hierarchy of existing models to rationalize the experimental observations [4, 19, 20]. Note that, as argued in the Supplemental Material, liquid inertia is negligible under realistic experimental conditions. The cartesian components

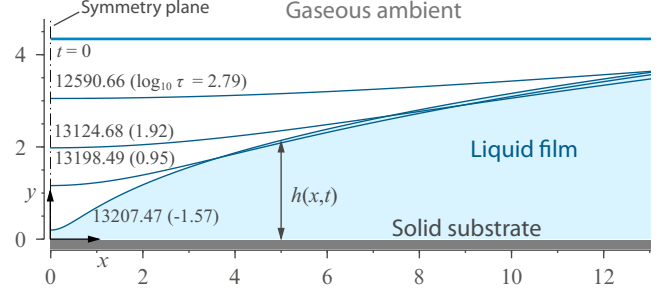


Figure 1. Schematics of the flow configuration, including a sample numerical evolution of the free surface for $h_o/a = 4.34$, where $a = [A/(6\pi\sigma)]^{1/2}$ is the molecular length scale [21]. The free-surface shapes are plotted at the four time instants indicated with blue dots in Fig. 2(b). The initial condition is $h_o/a(1 - 10^{-3} \cos 0.063x)$, with an associated rupture time $t_R \approx 1.3207501 \times 10^4$ (Fig. 2d).

of the liquid velocity field in the (x, y) directions are (u, v) , and the pressure field is p .

Dimensional analysis.— Dimensional arguments suggest the existence of a similarity solution of the Stokes equations near contact that differs from the lubrication result [14]. Indeed, the parametric dependences of the longitudinal velocity, transverse velocity, pressure and film thickness are

$$[u^*, v^*, p^*] = [F_u^*, F_v^*, F_p^*](x^*, y^*, \tau_*, \mu, A, \sigma, h_o), \quad (1)$$

$$h^* = F_h^*(x^*, \tau_*, \mu, A, \sigma, h_o), \quad (2)$$

where $\tau_* = t_R^* - t^*$ is the time remaining to rupture, and asterisks denote the dimensional versions of the flow variables. Taking (τ_*, μ, A) as dimensional basis, the Buckingham Π theorem provides the reduced functional dependences,

$$[u^*, v^*] = [\Pi_u, \Pi_v](\xi, \eta, \Pi_\sigma, \Pi_{h_o})(A/\mu)^{1/3} \tau_*^{-2/3}, \quad (3)$$

$$p^* = \Pi_p(\xi, \eta, \Pi_\sigma, \Pi_{h_o}) \mu \tau_*^{-1}, \quad (4)$$

$$h^* = \Pi_h(\xi, \Pi_\sigma, \Pi_{h_o})(A/\mu)^{1/3} \tau_*^{1/3}, \quad (5)$$

where $[\xi, \eta, \Pi_{h_o}] = (\mu/A)^{1/3} \tau_*^{-1/3} [x^*, y^*, h_o]$ and $\Pi_\sigma = \sigma/(A^{1/3} \mu^{2/3}) \tau_*^{2/3}$. When $\tau_* \rightarrow 0$, $\Pi_\sigma \rightarrow 0$ and $\Pi_{h_o} \rightarrow \infty$, suggesting that, as contact is approached, surface tension forces become negligible and the local flow becomes independent of h_o . Thus, we expect a local self-similar Stokes flow near rup-

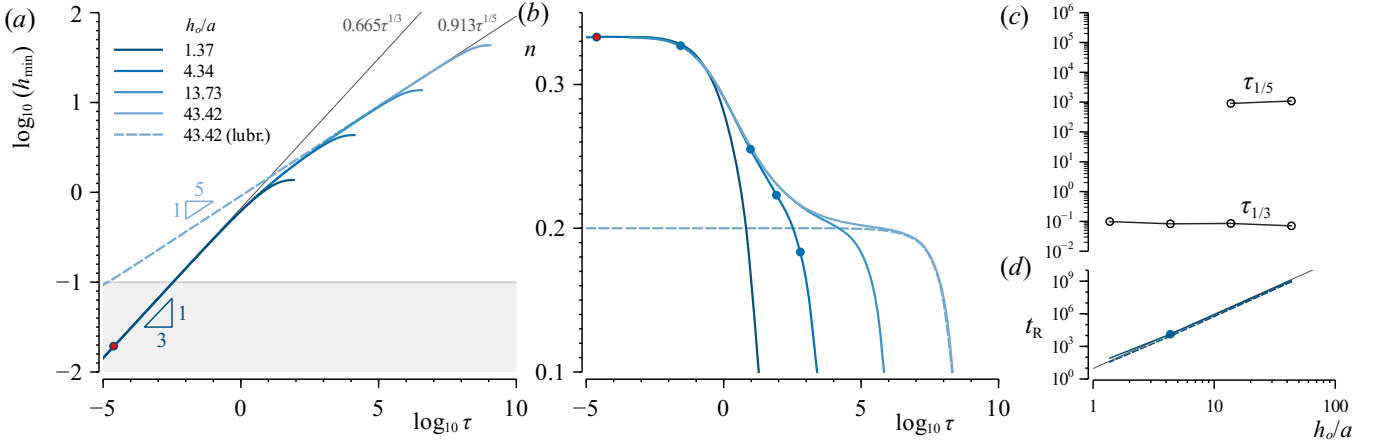


Figure 2. (a) Minimum film thickness as a function of the time remaining to rupture (solid lines) for $h_o/a = (1.37, 4.34, 13.73, 43.42)$ and initial conditions $h_o/a(1 - 10^{-3} \cos kx)$, using the corresponding optimal wavenumbers, $k = (0.17, 0.063, 0.021, 0.0065)$. The results obtained with the lubrication approximation [14] are also presented for $h_o/a = 43.42$ (dashed line). (b) Instantaneous exponent $n(\tau) = d \log_{10} h_{\min} / d \log_{10} \tau$. The blue dots indicate the times at which the interface profiles are plotted in Fig. 1, and the red dot marks the time chosen for the self-similarity test of Fig. 4. (c) Times at which $n(\tau_{1/5}) = 1/5 + 0.1 \times (1/3 - 1/5)$, and at which $n(\tau_{1/3}) = 1/5 + 0.9 \times (1/3 - 1/5)$, obtained from the Stokes equations. (d) Rupture time t_R obtained from the Stokes equations (solid line), from the lubrication equation (dashed line), and estimated from a linear stability of the lubrication equation (12) as $t_R \approx 4/3 \ln(10^3)(h_o/a)^5$ (thin line). The dot marks the rupture time associated with Fig. 1.

ture of the form

$$[u^*, v^*] \xrightarrow{\tau_* \rightarrow 0} [U(\xi, \eta), V(\xi, \eta)] (A/\mu)^{1/3} \tau_*^{-2/3}, \quad (6)$$

$$p^* \xrightarrow{\tau_* \rightarrow 0} P(\xi, \eta) \mu / \tau_*, \quad (7)$$

$$h^* \xrightarrow{\tau_* \rightarrow 0} H(\xi) (A/\mu)^{1/3} \tau_*^{1/3}. \quad (8)$$

Governing equations.— The molecular length scale [21], $a = [A/(6\pi\sigma)]^{1/2}$, is taken as the relevant characteristic length scale for the ultrathin liquid films considered in the present work, together with $\mu a/\sigma$, σ/μ and $A/(6\pi a^3)$ as time, velocity and pressure scales, respectively. The non-dimensional Stokes equations read

$$\nabla \cdot \mathbf{u} = 0, \quad 0 = -\nabla \phi + \nabla \cdot \mathbf{T}, \quad (9)$$

where $\mathbf{u} = (u, v)$, $\mathbf{T} = -p\mathbf{I} + \nabla \mathbf{u} + (\nabla \mathbf{u})^T$ is the liquid stress tensor and $\phi = h^{-3}$ is the dimensionless vdW potential. The accompanying boundary conditions include the non-slip condition $\mathbf{u} = 0$ at the solid wall $y = 0$ and

$$\mathbf{T} \cdot \mathbf{n} + (\nabla \cdot \mathbf{n}) \mathbf{n} = 0, \quad (10)$$

$$\mathbf{n} \cdot (d\mathbf{x}_s/dt - \mathbf{u}) = 0, \quad (11)$$

at the free surface $y = h(x, t)$, with corresponding parametrization \mathbf{x}_s and unit normal vector \mathbf{n} , accounting for the stress balance and the kinematics of the interface, respectively. In contrast with Stokes flow, the lubrication approximation provides the much simpler leading-order description

$$h_t + (h^3 h_{xxx}/3 + h^{-1} h_x)_x = 0, \quad (12)$$

governing the evolution of the free surface under the small-slope assumption [13, 14]. Hereafter, subscripts will denote partial derivatives. Note that the dimensionless initial film thickness, h_o/a , is the only governing parameter.

Flow evolution.— The equations of motion (9)–(11) were numerically integrated with the initial condition $\mathbf{u} = 0$ and $h(x, 0) = h_o/a(1 - 10^{-3} \cos kx)$ for $0 < x < \pi/k$, where k was chosen as the wavenumber of maximum amplification deduced from a linear stability analysis of (9)–(11), not reported here for conciseness. The additional symmetry conditions $u = v_x = 0$ are imposed at the planes $x = 0$ and $x = \pi/k$. A detailed description of the numerical techniques can be found in the Supplemental Material. A representative numerical integration is presented in Fig. 1 for $h_o/a = 4.34$. The slightly disturbed flat film profile departs from the initial condition by virtue of the destabilizing vdW forces in a self-accelerated process, leading to a rupture singularity in a finite time t_R , whose precise computation involved an algebraic fitting procedure that took advantage of the anticipated power-law behavior $h_{\min} \propto \tau^{1/3}$ for $\tau \rightarrow 0$. Sample computations are depicted in Fig. 2 for several values of h_o/a . The accompanying instantaneous exponent $n = d \log_{10} h_{\min} / d \log_{10} \tau$ reveals the persistent self-similar behavior $h_{\min} \rightarrow K_S \tau^{1/3}$ for $\tau \lesssim 0.1$ and all values of h_o/a , in agreement with dimensional analysis, where $K_S = 0.665$. The solution of the lubrication equation (12) for $h_o/a = 43.42$ (dashed line) also exhibits a self-similar behavior [14], but with a different asymptotic law $h_{\min} \rightarrow K_L \tau^{1/5}$, where $K_L = 0.913$. The crossover time between the lubrication and Stokes self-similar solutions can be estimated by equating $K_L \tau_c^{1/5} = K_S \tau_c^{1/3} \Rightarrow \tau_c = (K_L/K_S)^{15/2} = 10.77$, with an associated minimum thickness $h_{\min,c} = K_S (K_L/K_S)^{5/2} = 1.47$. Indeed, the results of Fig. 2 for $h_o/a = 43.42$ reveal that the evolution of $h_{\min}(\tau)$ obtained with the lubrication equation closely follows the Stokes result for $\tau \geq \tau_{1/5} \approx 10^3$ with a scaling exponent of $1/5$, followed by a long crossover for $\tau_{1/3} \leq \tau \leq \tau_{1/5}$, and finally reaching the $1/3$ power law for $\tau \leq \tau_{1/3} \approx 0.08$. In terms of the minimum

film thickness, the $1/5$ -scaling takes place for $h_{\min} \geq 3.63$, the crossover for $0.29 \leq h_{\min} \leq 3.63$, and the $1/3$ -scaling for $h_{\min} \leq 0.29$. The failure of lubrication theory to predict the last stages of the rupture behavior observed in Fig. 2 demands unraveling the local self-similar Stokes flow.

Self-similar solution.— Dimensional analysis suggests substituting the similarity ansatz

$$\begin{aligned} x &= \tau^{1/3} \xi, \quad y = \tau^{1/3} \eta, \quad h = \tau^{1/3} f(\xi), \quad u = \tau^{-2/3} U(\xi, \eta), \\ v &= \tau^{-2/3} V(\xi, \eta), \quad p = \tau^{-1} P(\xi, \eta) \end{aligned} \quad (13)$$

into (9)–(11) to elucidate the structure of the leading-order flow for $\tau \rightarrow 0$. The self-similar Stokes equations read

$$U_\xi + V_\eta = 0, \quad (14)$$

$$U_\xi \xi + U_\eta \eta = P_\xi - 3f^{-4} f_\xi, \quad (15)$$

$$V_\xi \xi + V_\eta \eta = P_\eta, \quad (16)$$

which must be integrated in $0 < \xi < \infty$, $0 < \eta < f(\xi)$, with the boundary conditions $U = V = 0$ at the wall $\eta = 0$, $U = V_\xi = 0$ at the symmetry plane $\xi = 0$, $0 < \eta < f(0)$, and

$$(1 + f_\xi^2)P - 2V_\eta + 2(V_\xi - f_\xi U_\xi + U_\eta)f_\xi = 0, \quad (17)$$

$$(1 - f_\xi^2)(V_\xi + U_\eta) + 2(V_\eta - U_\xi)f_\xi = 0, \quad (18)$$

$$f/3 - (\xi/3 + U)f_\xi + V = 0, \quad (19)$$

at the unknown free surface $\eta = f(\xi)$. Notice that the leading-order contribution of the normal component of (10) is $O(\tau^{-1})$, while the capillary pressure is $O(\tau^{-1/3})$. Thus, as anticipated by dimensional arguments, surface tension does not contribute to the normal-stress equilibrium at leading order as $\tau \rightarrow 0$. The system of nonlinear elliptic PDEs (14)–(19) describing the local Stokes flow close to rupture is parameter-free. It is interesting to note that problems with similar mathematical structure appear in other free-surface flows like inertial focusing and jet breakup [15, 17]. The asymptotic description of film rupture is completed by specifying the far-field boundary conditions at $\xi^2 + \eta^2 \gg 1$, $0 < \eta < f(\xi)$. Inspection of the kinematic boundary condition (19) reveals that $f \propto \xi$ for $\xi \gg 1$ if U and V are subdominant. This suggests that the shape of the free surface sufficiently far from the origin, $r \gg 1$, is a wedge $\theta = \theta_o$, where (r, θ) are polar coordinates such that $\xi - \xi_o = r \cos \theta$ and $\eta = r \sin \theta$, and (V_r, V_θ) are the associated radial and polar components of the velocity field. Insight of the far-field behavior was first obtained by numerically integrating (14)–(19) imposing a stress-free boundary condition sufficiently far from the origin, as explained in the Supplemental Material together with a detailed description of the numerical technique employed. The examination of the radial and polar velocity profiles along rays $\theta = \text{constant}$ revealed that $V_r \sim V_\theta \sim r^{-(1+\lambda)}$ for $r \gg 1$, where λ is a positive constant smaller than unity. This suggests a far-field stream function of the form [22] $\psi = F(\theta)/r^\lambda$, such that $V_r = r^{-1} \partial \psi / \partial \theta = F' r^{-(1+\lambda)}$ and $V_\theta = -\partial \psi / \partial r = \lambda F r^{-(1+\lambda)}$. Since ψ is biharmonic, F is seen to be the solution to the fourth-order linear homogeneous equation

$$F^{(iv)} + [4 + 2\lambda(2 + \lambda)]F'' + \lambda^2(2 + \lambda)^2 F = 0, \quad (20)$$

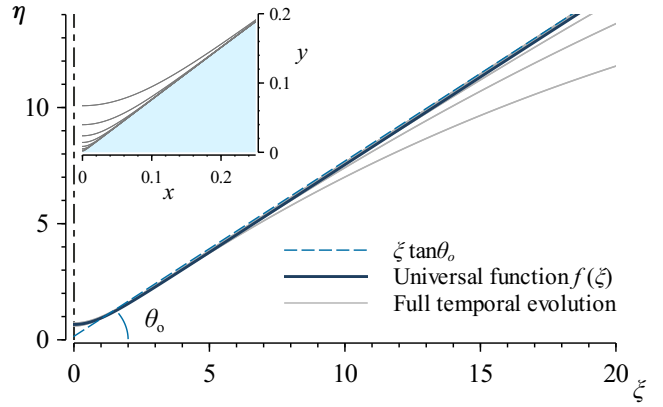


Figure 3. Comparison of the function $f(\xi)$ obtained from the self-similar solution (thick solid line) with eight rescaled profiles obtained from the numerical simulations for $h_o/a = 4.34$ at times $-\log_{10} \tau = (2.98, 3.66, 4.33, 5.00, \dots, 7.75)$ (thin solid lines). The asymptotic shape $\xi \tan \theta_o$, with $\theta_o = 37^\circ$ (dashed line) is plotted with a vertical offset of 0.15. The inset shows the unscaled profiles.

with the no slip condition $F = F' = 0$ at $\theta = 0$, and the vanishing normal, $F''' + [4 + 3\lambda(2 + \lambda)]F' = 0$ and tangential, $F'' - \lambda(2 + \lambda)F = 0$ stress boundary conditions at $\theta = \theta_o$. If λ were known, Eq. (20) together with the boundary conditions discussed above would constitute a closed eigenvalue problem for the universal angle θ_o . However, λ is expected to be determined from the asymptotic matching with a near-field description for $\xi \ll 1$, which is beyond the scope of this work. We propose the following alternative: nontrivial solutions to (20) satisfying the boundary conditions exist if

$$(\lambda + 1)^2 \cos(2\theta_o) + \cos[2\theta_o(\lambda + 1)] - \lambda(\lambda + 2) = 0, \quad (21)$$

which determines the pairs (θ_o, λ) classifying the family of allowed far-field solutions of the Stokes equations with a free-surface angle θ_o . Thus one may i) extract θ_o from a numerical integration of (14)–(19) with a stress-free far-field boundary condition and then obtain λ from (21) and ii) repeat the integration now imposing the far field variables entailed in the description of F . This iterative process converges very fast, and is stopped when the successive values of θ_o differ less than a prescribed tolerance. The universal function $f(\xi)$ is represented in Fig. 3 together with rescaled film profiles $h/\tau^{1/3}$ for $h_o/a = 4.34$, along with the far-field behavior $f = \xi \tan \theta_o$. The local expansion of the function f for $\xi \ll 1$ has the form $f = f(0) + f''(0)\xi^2 + \mathcal{O}(\xi^4)$ due to the symmetry of the interface, with coefficients $f(0) = 0.66$ and $f''(0) = 0.59$. As a final self-similarity test, Fig. 4 displays isocontours of $U(\xi, \eta)$ obtained from the solution of (14)–(19) (right), and from the temporal integration of (9)–(11) for $\log_{10} \tau = -4.62$ (left), while the inset shows the corresponding profiles of x - and y -velocity along the interface.

Realizability of the self-similar regimes.— The self-similar lubrication and Stokes regimes prevail for $h_{\min}(\tau_{1/5}) > 3.63$ and $h_{\min}(\tau_{1/3}) < 0.29$, the latter values corresponding to dimensional minimum thicknesses of $h_{\min}^* > 3.63a$ and $h_{\min}^* <$

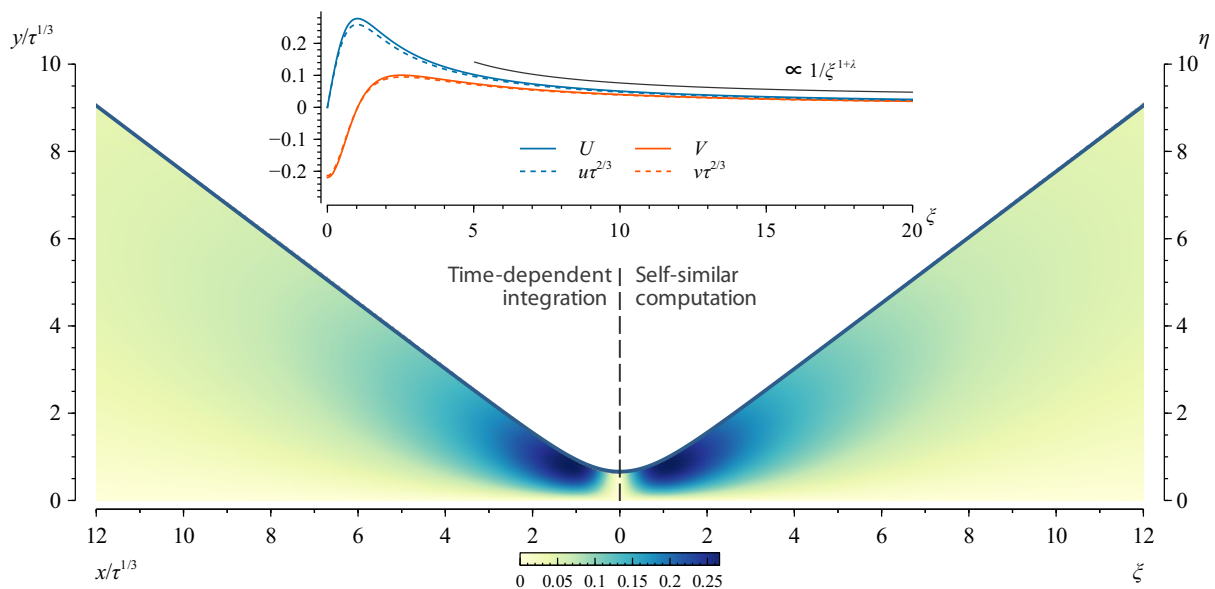


Figure 4. Isocontours of U obtained by solving the self-similar system (14)–(19) (right panel), and by using the rescaled velocity $u\tau^{2/3}$ for $\log_{10}\tau = -4.62$ extracted from the simulation of (9)–(11) (left panel; red dot in Fig. 1). The inset shows the values of U and V along the interface, together with the asymptotic far-field law $\xi^{-(1+\lambda)}$ for $\xi \gg 1$.

0.29 a , respectively. Taking, for instance, $A = 2.2 \times 10^{-20}$ J, $\sigma = 3.8 \times 10^{-2}$ Jm $^{-2}$ as representative values for ultrathin polymer films [5] provides $a = 1.75$ Å. For $h_o = 4$ nm [5], the value of $h_o/a = 22.82$ which, according to Fig. 2(b), corresponds to a case where the self-similar lubrication regime is not established. The self-similar Stokes regime would be reached for $h_{\min}^* < 0.5$ Å, at which the continuum description is not valid. More importantly, short-range intermolecular forces, not taken into account in the present analysis, would become important at larger values of h_{\min}^* . It is therefore concluded that, in the case of ultrathin polymer films, neither self-similar regime is experimentally realized.

Concluding remarks.– The self-similar solution obtained herein under Stokes flow arises from the same balance between viscous and vdW forces as in the lubrication theory of Zhang and Lister [14]. The failure of the slender description to account for the flow structure near breakup is due to the fact that $\tan\theta_o \approx 0.75 \sim 1$. Indeed, the far-field shape of the interface is $f \rightarrow \xi^{1/2}$ according to [14], while we have shown that $f \rightarrow \xi$. Although the leading-order lubrication theory does not describe the vdW-induced rupture of thin films correctly, a higher-order theory might yield more accurate results [23]. It is important to note that, regardless of the self-similar nature of the rupture dynamics, lubrication theory predicts an evolution for the liquid film that is markedly different from the Stokes description, as clearly evidenced by Fig. 2. Indeed, this difference appears during the early stages after the onset of the vdW instability, and increases over time. In particular, the 1/5 power law predicted by lubrication theory is only accomplished transiently during a very short intermediate time interval prior to the crossover to the 1/3 power law

described here for the first time.

Future prospects.– Natural extensions of our work include for instance the effect of wall slip [24], the study of axisymmetric rupture [14, 25], the breakup of free films [26–28], the influence of surfactants [29, 30], liquid-liquid dewetting [31–33], the influence of polymer rheology [9], and the effect of thermal noise [34–37]. Of particular importance is the inclusion of more detailed models of intermolecular interactions [4, 19, 20, 38], as required to account for the resulting dewetting patterns and their long-term coarsening [5, 39].

The authors thank J. Rivero-Rodríguez and B. Scheid for key numerical advice, A.L. Sánchez, C. Martínez-Bazán and J.M. Gordillo for their enduring teaching and encouragement, W. Coenen for carefully reading the manuscript, and H.A. Stone for sharing his insights, and for his kind hospitality at the Complex Fluids Group, Princeton. This research was funded by the Spanish MINECO, Subdirección General de Gestión de Ayudas a la Investigación, through project DPI2015-71901-REDT, and by the Spanish MCIU-Agencia Estatal de Investigación through project DPI2017-88201-C3-3-R, partly financed through FEDER European funds. A.M.-C. also acknowledges support from the Spanish MECD through the grant FPU16/02562 and to its associated program Ayudas a la Movilidad 2018 during his stay at Princeton University.

* Corresponding author: alejandro.sevilla@uc3m.es

[1] F. B. Wyart and J. Dailant, *Can. J. Phys.* **68**, 1084 (1990).
[2] G. Reiter, *Phys. Rev. Lett.* **68**, 75 (1992).

- [3] A. Oron, S. H. Davis, and S. G. Bankoff, *Rev. Mod. Phys.* **69**, 931 (1997).
- [4] R. Seemann, S. Herminghaus, and K. Jacobs, *Phys. Rev. Lett.* **86**, 5534 (2001).
- [5] J. Becker, G. Grün, R. Seemann, H. Mantz, K. Jacobs, K. R. Mecke, and R. Blossey, *Nat. Mater.* **2**, 59 (2003).
- [6] U. Thiele, in *Thin films of soft matter* (Springer, 2007), pp. 25–93.
- [7] R. Craster and O. Matar, *Rev. Mod. Phys.* **81**, 1131 (2009).
- [8] D. Bonn, J. Eggers, J. Indekeu, J. Meunier, and E. Rolley, *Rev. Mod. Phys.* **81**, 739 (2009).
- [9] R. Blossey, *Thin liquid films: dewetting and polymer flow* (Springer Science & Business Media, 2012).
- [10] A. Scheludko, *Proc. Koninkl. Ned. Akad. Wet. B* **65**, 86 (1962).
- [11] A. Vrij, *Discussions of the Faraday Society* **42**, 23 (1966).
- [12] E. Ruckenstein and R. K. Jain, *J. Chem. Soc., Faraday Trans. 2* **70**, 132 (1974).
- [13] M. B. Williams and S. H. Davis, *J. Colloid Interface Sci.* **90**, 220 (1982).
- [14] W. W. Zhang and J. R. Lister, *Phys. Fluids* **11**, 2454 (1999).
- [15] D. T. Papageorgiou, *J. Fluid Mech.* **301**, 109 (1995).
- [16] R. F. Day, E. J. Hinch, and J. R. Lister, *Phys. Rev. Lett.* **80**, 704 (1998).
- [17] B. W. Zeff, B. Kleber, J. Fineberg, and D. P. Lathrop, *Nature* **403**, 401 (2000).
- [18] H. Hamaker, *Physica* **4**, 1058 (1937).
- [19] U. Thiele, M. G. Velarde, and K. Neuffer, *Phys. Rev. Lett.* **87**, 016104 (2001).
- [20] J. N. Israelachvili, *Intermolecular and surface forces* (Academic press, 2011).
- [21] P.-G. De Gennes, *Rev. Mod. Phys.* **57**, 827 (1985).
- [22] G. Barenblatt and Y. B. Zel'Dovich, *Annu. Rev. Fluid Mech.* **4**, 285 (1972).
- [23] C. Ruyer-Quil and P. Manneville, *Eur. Phys. J. B* **15**, 357 (2000).
- [24] D. Peschka, S. Haefner, L. Marquant, K. Jacobs, A. Münch, and B. Wagner, *Proc. Natl. Acad. Sci.* **116**, 9275 (2019).
- [25] T. P. Witelski and A. J. Bernoff, *Physica D: Nonlinear Phenomena* **147**, 155 (2000).
- [26] A. Vrij and J. T. G. Overbeek, *J. Am. Chem. Soc.* **90**, 3074 (1968).
- [27] D. Vaynblat, J. R. Lister, and T. P. Witelski, *Phys. Fluids* **13**, 1130 (2001).
- [28] L. Champougny, E. Rio, F. Restagno, and B. Scheid, *J. Fluid Mech.* **811**, 499 (2017).
- [29] D. A. Edwards and A. Oron, *J. Fluid Mech.* **298**, 287 (1995).
- [30] M. Warner, R. Craster, and O. Matar, *Phys. Fluids* **14**, 4040 (2002).
- [31] F. B. Wyart, P. Martin, and C. Redon, *Langmuir* **9**, 3682 (1993).
- [32] A. Pototsky, M. Bestehorn, D. Merkt, and U. Thiele, *Phys. Rev. E* **70**, 025201 (2004).
- [33] M. H. Ward, *Phys. Fluids* **23**, 062105 (2011).
- [34] B. Davidovitch, E. Moro, and H. A. Stone, *Phys. Rev. Lett.* **95**, 244505 (2005).
- [35] G. Grün, K. Mecke, and M. Rauscher, *J. Stat. Phys.* **122**, 1261 (2006).
- [36] R. Fetzer, M. Rauscher, R. Seemann, K. Jacobs, and K. Mecke, *Phys. Rev. Lett.* **99**, 114503 (2007).
- [37] S. Nestic, R. Cuerno, E. Moro, and L. Kondic, *Phys. Rev. E* **92**, 061002 (2015).
- [38] A. A. Pahlavan, L. Cueto-Felgueroso, A. Hosoi, G. McKinley, and R. Juanes, *J. Fluid Mech.* **845**, 642 (2018).
- [39] K. B. Glasner and T. P. Witelski, *Phys. Rev. E* **67**, 016302 (2003).